scientific reports

Check for updates

OPEN

SH-SSQ as a modifier for superior mechanical properties and improved plasticity of 3D printed PLA

Bogna Sztorch[1]✉, Daria Pakuła[1], Miłosz Frydrych[1]✉, Eliza Romańczuk-Ruszuk[2], Tomasz Osiecki[3], Holger Sedlitz[3] & Robert E. Przekop[1]

This work confirms that the use of silisequioxanes in the modification of polymeric and composite materials to change their properties is possible in the range of low modifier concentrations, not exceeding 2.5%. This study investigates the impact of (3-thiopropyl)polysilsesquioxane (SSQ-SH) on the properties of polylactide (PLA) for 3D printing. Microscopic analysis using SEM and EDS mapping proved that SSQ-SH is well dispersed in the polymer matrix in the concentration range of 0.25–2.5 wt%, agglomerations were observed at 5 wt% concentration, which reduces the homogeneity of the material and is also reflected in the mechanical test results. Mechanical testing shows SSQ-SH enhances flexibility and toughness, with the most significant improvements observed at 1 wt% and 1.5 wt% concentrations. Specifically, elongation at break increases by up to 56% and impact strength by up to 37% compared to unmodified PLA. These results suggest SSQ-SH is an effective plasticizer, improving interlayer adhesion and reducing brittleness. The optimal SSQ-SH concentrations for maximizing mechanical performance and material integrity are 1 wt% and 1.5 wt%. Part of the produced samples was conditioned in a climatic chamber, it was observed based on DSC and XRD analysis that the crystallinity of the materials significantly increases after exposure to UV radiation, which is also confirmed by microscopic observations. This study highlights the potential of SSQ-SH in improving the performance of 3D printed PLA materials and efficient modification is possible even in the range of low modifier concentrations, not exceeding 2.5%.

Keywords Octa(3-thiopropyl)silsesquioxanes, PLA, Polylactide, 3D printing

The global polymer market was worth USD 712 billion in 2023, and forecasts indicate that over the next 10 years, its value may reach up to USD 1050 billion (statistica.com). The growth in demand for polymers is driven mainly by growing sales of consumer products, in which these materials play a key role[1]. Polylactide (PLA), which is a polyester polymer derived from renewable resources, is attracting increasing interest in the plastics sector, due to its favorable mechanical and thermal properties and biocompatibility, as well as biodegradability, it has become an attractive alternative to traditional petroleum-based polymers[2,3]. However, despite many advantages that may constitute an advantage over other popularly used polymers, PLA also has some limitations that pose a challenge in some specialized applications. One of the key problems is its high brittleness, which translates into low-impact strength[4,5]. Therefore, PLA is the subject of intense scientific research and industry interest, which are aimed at improving these parameters to expand the scope of its applications. Polylactide is one of the most frequently used materials in additive technologies using thermoplastic polymers as the building material[6]. Fused fabrication filament/fused deposition modeling (FFF/FDM) technology allows one to create tridimensional objects by applying subsequent layers of material "layer by layer", directly based on data from CAD files[7,8]. Its significant advantage is the lack of release of toxic waste during the printing process and much easier processability resulting from low thermal shrinkage and relative resistance to changes in ambient temperature[9]. Due to the possibility of producing more complicated and complex objects compared to traditional processing methods[10], as well as the possibility of rapid prototyping while limiting the time[11,12] and, above all, the cost of

[1]Centre for Advanced Technologies, Adam Mickiewicz University Poznan, 61-614 Poznań, Poland. [2]Institute of Biomedical Engineering, Faculty of Mechanical Engineering, Bialystok University of Technology, Wiejska 45C, 15-351 Bialystok, Poland. [3]Brandenburg Technical University Cottbus-Senftenberg, 03046 Cottbus, Germany. ✉email: bogna.sztorch@amu.edu.pl;

the process[13], 3D printing is one of the most significant new generation industry technologies[14,15]. 3D printing eliminates the need to design and make tools such as injection molds, which shortens production time and costs. This process allows objects to be produced within a few hours, from design to finished product, which is a big advantage in terms of low-volume production over traditional methods. Moreover, during 3D printing, only the material necessary to produce the final product is used, which minimizes material losses[16]. Elements manufactured using 3D technology are often characterized by lower mechanical strength, which results from problems with poor interlayer adhesion, the presence of air gaps, and deformations[17]. Additive technologies such as FDM have many advantages but still require research and development to improve production processes and modify materials to obtain better results.

Recently, there has been a growing interest in organosilicon compounds acting as modifiers and nanofillers in plastics[18–20]. The introduction of these compounds into the polymer can significantly affect various properties of the material, such as rheology[21] and hydrophobicity[22,23], thermal stability[24]. Adding silsesquioxanes to plastics significantly improves mechanical strength, stiffness, and wear resistance[25–27]. They can also increase melting point and thermal stability[28], making them suitable for producing high-temperature materials such as heat insulators, electronic device housings, and components operating in harsh environments. Thanks to their chemical resistance, SSQs can effectively protect plastics against aggressive chemicals[29]. Silsesquioxanes, which can be substituted with various types of functional groups, can give plastics different properties, depending on their final purpose.

Polylactide and silsesquioxane nanocomposites are increasingly utilized in additive manufacturing technologies. Research conducted by Meyva-Zeybek et al. compared the properties of PLA/OctaIsobutylsilsesquioxane (SSQ) nanocomposites produced via 3D printing with PLA/SSQ samples formed by compression molding. Due to the superior homogeneity and more uniform distribution of POSS nanoparticles within the PLA matrix layers, mechanical testing (tensile, flexural, and impact) revealed significantly higher values of strength, modulus of elasticity, and fracture resistance for the 3D-printed samples compared to those formed by compression molding. The enhancement in these properties ranged from 13 to 78%[30]. Another research area is the biomedical application of nanocomposites. Nasma Anjrini et al. demonstrated the potential to fabricate scaffolds based on PLA/polymethyl silsesquioxane (PMSQ) coated with vitamin E microparticles using 3D printing technology and electrospinning methods. The mechanical, thermal, chemical, morphological, and biological properties of these scaffolds were thoroughly analyzed. The biocompatibility studies revealed that the scaffolds were not cytotoxic. SEM analysis disclosed a uniform morphology of the 3D-printed scaffolds[31]. In our previous work, we explored the management of rheological and mechanical parameters of PLA-based composites using cubic organofunctional silsesquioxane structures. It was observed that the addition of silsesquioxanes with alkoxy and alkyl groups provides a lubricating effect for the molten polymer under load, as well as possesses plasticizing properties[21]. We also presented findings on the use of a limonene-derived silsesquioxane as a modifier for polylactide in 3D printing and injection molding applications. Based on the data obtained, it can be concluded that the addition of the functionalized silsesquioxane significantly enhances parameters such as tensile strength, flexural strength, and impact resistance of 3D-printed samples. Additionally, this modifier facilitates the printing process itself, improving rheological properties (reducing viscosity and increasing melt flow rate) and reducing production waste[32].

Despite the existing literature, there is still an urgent need to develop new modifiers that affect the properties of polylactide. It is important to develop systems with good mechanical properties that will eliminate such features of polylactide as brittleness and processability, while being effective at low concentrations. The development of composites with good mechanical properties significantly expands the possibilities of their application, especially in the context of utility materials and spare parts, which is currently one of the key applications of additive technologies. This study presents new nanomaterials based on PLA modified with (3-thiopropyl) polysilsesquioxane, specially adapted to FDM printing technology. Comprehensive studies were carried out, including microscopic analysis, mechanical tests and thermal analyses.

Materials and methods

Materials

Polylactide (PLA) type Ingeo 2003D was purchased from NatureWorks, MFR = 6 g/10 min (210, 2,16 kg), specific gravity 1.24, melting temperature 210 °C, Tensile Strength 7.700 MPa, tensile modulus 500 GPa.

The chemicals were purchased from the following sources 3-Mercaptopropyltrimethoxysilane (99%) from BRB International BV, methanol p.a. from P.P.H Stanlab; hydrochloric acid (35–38%), toluene, tetrahydrofuran, dichloromethane from Chempur, chloroform-d from Merck S.A.

Procedure for synthesis of (3-thiopropyl)polysilsesquioxane

(3-thiopropyl)polysilsesquioxane (SSQ-SH) was prepared according to the literature [33,34]. SSQ-SH is an amorphous hydrolytic condensation product of 3-mercaptoropyltrimethoxysilane (Fig. 1). The ^{29}Si NMR present shifts at -56.37-(-60.38) ppm (Si–OH), -64.42-(-67.15) ppm (Si–O-Si). Detailed physicochemical characterization of silsesquioxane was presented in our previous article[35].

Preparation of samples

Preparation of PLA/SSQ-SH filaments

PLA 2003D and SSQ-SH were homogenized using a laboratory two-roll mill ZAMAK MERCATOR WG 150/280. A portion of 500 g PLA Ingeo™ 2003 D was mixed with the chemical modifier SSQ-SH, until the final concentration of the additive of 5.0 wt%. The mixing was performed for 15 min when the rolls' temperature reached 210 °C until full homogeneity of the concentrates. Masterbatch was granulated by a WANNER C17.26 grinding mill. The granulate was diluted with neat PLA up to the final filler concentrations of wt. 0. 25%, 0.5%,

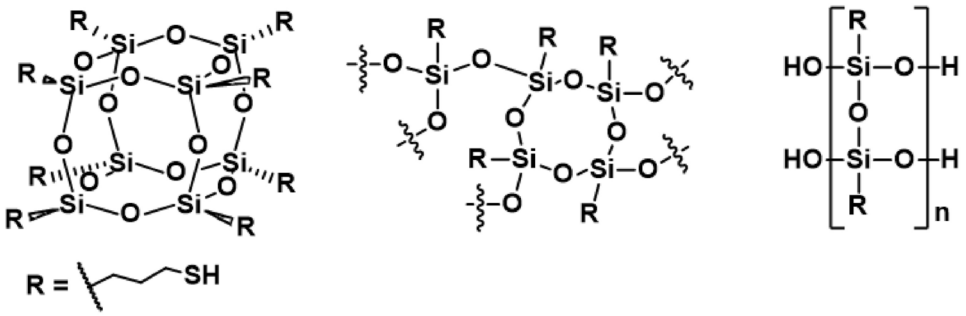

Fig. 1. The mixture of the different structures of (3-thiopropyl)polysilsesquioxane.

Nozzle diameter	0.4 mm
Extruder temperature	180 °C
Layer height	0.18 mm
Bottom and top layers number	3
Infill pattern	Linear
Fill angle	45°
Infill density	100%
Printing speed	120 mm/s

Table 1. The parameters of the printing process.

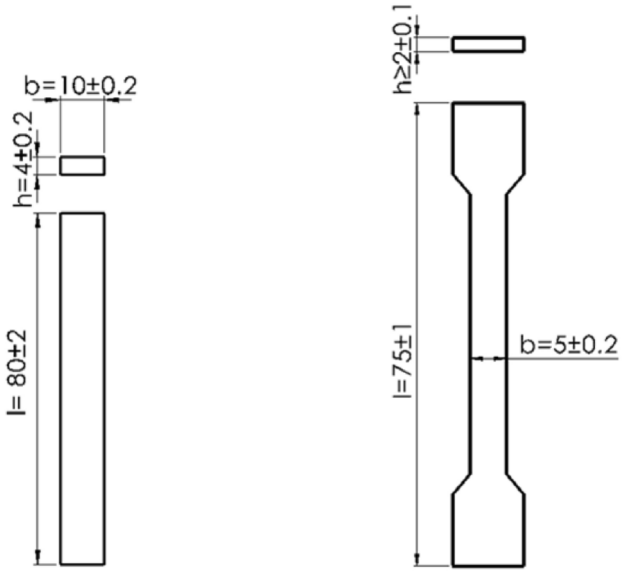

Fig. 2. Dimensions of samples used for the mechanical tests.

1.0%, 1.5%, and 2.5% upon extrusion moulding of a stream with four heating zones nozzle (190 °C), zone 3 (200 °C), zone 2 (195 °C) and zone 1 (190 °C), with consequent cold granulation on the HAAKE Rheomex OS single-screw extrusion setup line, and then dried for 24 h at 50 °C. The filament was obtained with a diameter of 1.75 mm on a Filabot EX6 single-screw extruder with four heating zones: nozzle (170 °C), zone 3 (185 °C), zone 2 (180 °C), and zone 1 (60 °C), an L/D 24 screw.

3D printing (FDM)

The filaments were used for the FFF 3D printing process. Two samples were printed using the Prusa i3 MK3S+3D printer: dumbbells and bars, according to PN-EN-ISO 527-2 (Table 1, Fig. 2).

Analyses
All analyses and processes were conducted under a temperature 20 °C.

Morphology and structure observation
SEM microphotographs of the breakthroughs after the impact test and SEM–EDS elemental analysis of the distribution of organosilicon modifier in the materials by S and Si mapping were taken using a Quanta FEG 250 (FEI) high-resolution scanning electron microscope.

Surface structure and breakthroughs were analysed under a Digital Light Microscope Keyence VHX 7000 with 100× to 1000× VH-Z100T lens (Osaka, Japan). All the pictures were recorded with a VHX 7020 camera.

Thermal analysis
Differential scanning calorimetry (DSC) was performed using a NETZSCH204 F1 Phoenix calorimeter Samples of 6±0.2 mg were placed in an aluminum crucible with a punctured lid. The measurements were performed under nitrogen in the 20–220 °C temperature range and at a 10 °C/min heating rate.

Mechanical properties
A Charpy impact test (with no notch) was performed on an Instron Ceast 9050 impact machine according to ISO 179–135. For impact strength tests, the obtained materials were printed into dumbbell specimens of type 1B following PN-EN ISO 527-1:2020-0133 and PN-EN ISO 178:2019-06.

For flexural and tensile strength testing, specimens were 3D printed with dimensions in accordance with the requirements of PN-EN ISO 178 and PN-EN ISO 527. The experiments were conducted according to the listed standards. Tests of the obtained specimens were performed on an INSTRON 5969 universal testing machine with a maximum load force of 50 kN. The traverse speed for tensile strength measurements was set at 2 mm/min.

UV aging/test chamber
All samples were subjected to an accelerated aging test in an ATLAS UV TEST weathering station. The UV-radiation aging tests have been carried out following ISO 4892-3 standard. A 500 h aging process was conducted under 0.76 W/m^2 UV-B fluorescent lamps irradiance at 313 nm wavelength, exposure cycle no.4, method C of PN-EN ISO 16474-3 standard in two alternating cycles of exposure of the materials to UV radiation at 60 °C for 4 h (light cycle) and condensation at 50 °C for 4 h (no UV radiation—dark cycle).

Fourier Transform-Infrared (FT-IR) spectra were recorded on a Nicolet iS 50 Fourier transform spectrophotometer (Thermo Fischer Scientifin) equipped with a diamond ATR unit with a resolution of 0.09 cm^{-1}.

X-Ray Diffraction (XRD: X-Ray Diffraction) was performed using a powder diffractometer (SmartLab Rigaku, Japan) with a CuK alpha lamp, in the range of 3-100 (2 thetas), scan step 0.01, scan speed 4o/min. Crystallinity was calculated from the formula[36]:

$$Crystallinity\ [\%] = \frac{Area\,of\,crystalline\,peaks}{Area\,of\,all\,peaks} \cdot 100$$

Results and discussion
Morphology and structure observation
SEM–EDS

The miscibility study of (3-thiopropyl)polysilsesquioxane with the polylactide matrix and the dispersion analysis of the additive in the polymer matrix was conducted using scanning electron microscopy with SEM–EDS mapping. Microscopic observations indicate that in systems containing 0.25 wt% of the modifier, SSQ-SH is well-dispersed and does not form agglomerates (Fig. 3A). For polymers containing 0.5–2.5 wt% SSQ-SH, despite the presence of small aggregates, a continuous phase of the polymer matrix saturated with well-dispersed additives was also observed. This suggests proper miscibility of the modifier with the polymer matrix, despite the formation of small aggregates, approximately 8 um in size. (Fig. 3B-E). This indicates that at these concentrations (0.5–2.5 wt%), SSQ-SH, although forming some agglomerates, still effectively mixes with polylactide, maintaining structural homogeneity at the microscopic level, for the system containing 5 wt% SSQ-SH/PLA (Fig. 3F), a significant decrease in homogeneity and an increase in the number and size of (3-thiopropyl) polysilsesquioxane agglomerates were observed. It is worth noting that the Si agglomerates form longitudinal bands as the concentration increases, the width was approximately 23 µm for the sample with 5 wt% SSQ-SH/PLA. This indicates limited miscibility of SSQ-SH at higher concentrations with the PLA matrix, resulting from the increased amount of the additive, which exceeds the capacity for uniform dispersion within the material structure. High additive concentration leads to the formation of large agglomerates, negatively impacting the mechanical properties of the material[37].

Optical microscopy

In the microscopic images (Fig. 4), the surface and fracture morphologies of the printed objects are presented. The addition of SSQ-SH influences the interlayer melting properties, the formation of defects such as voids, and their mechanical damage (brittle fracture, plastic fracture), which consequently affect the mechanical strength of the samples under load. Unmodified polylactide exhibits moderate melting between the individual layers. Additionally, brittle fractures and interlayer voids are formed. The addition of SSQ-SH in low concentrations, namely 0.25 wt% and 0.5 wt%, does not significantly affect the material's melting. At 1 wt% modifier content, a plasticizing effect is observed within the fractured material, resulting in a reduction of defects and better interlayer

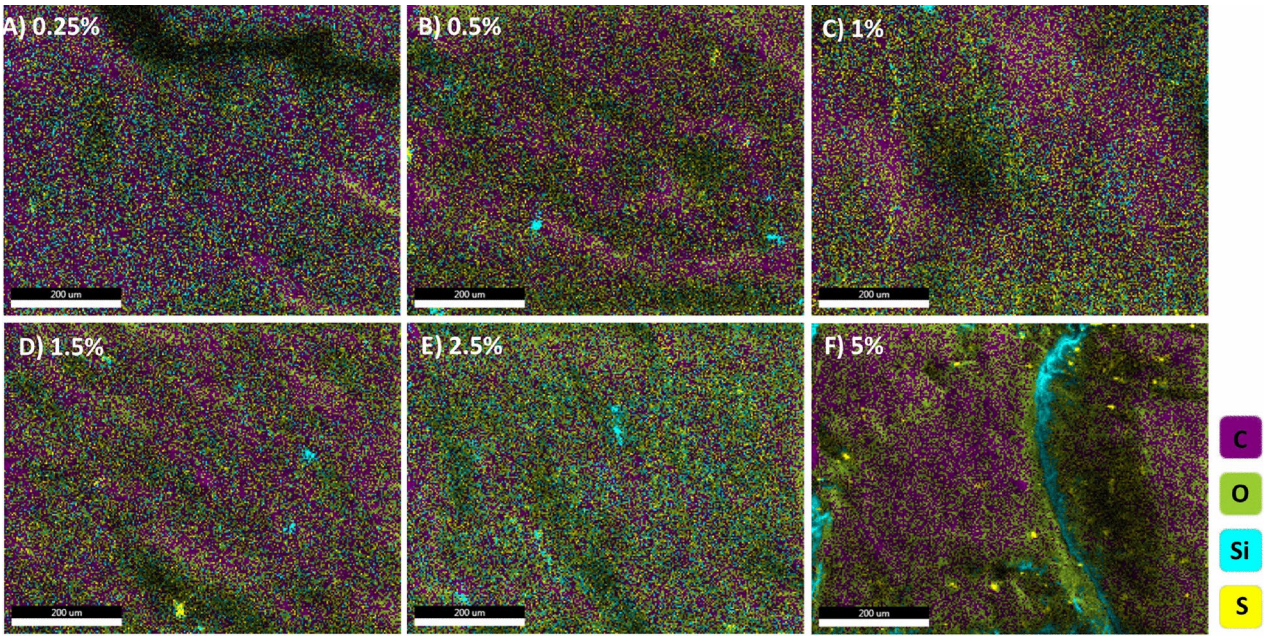

Fig. 3. Dispersion analysis in a polylactide matrix containing different wt% of modifier: (**A**) 0.25%, (**B**) 0.5%, (**C**) 1%, (**D**) 1.5%, (**E**) 2.5%, (**F**) 5%.

melting of the print. Images of the 5 wt% SSQ-SH/PLA show a significant change in the sample structure. At this modifier concentration, the material exhibits more uniform melting between layers. Notably, there is a decrease in the number of voids and an improvement in material cohesion, indicating potentially enhanced mechanical properties of the modified PLA under load. Furthermore, the SSQ-SH additive at higher concentrations (e.g. 5 wt%) appears to facilitate the formation of a more continuous phase within the polymer matrix, promoting stronger interlayer adhesion. This analysis highlights the importance of optimizing the concentration of SSQ-SH to achieve the desired balance between enhanced mechanical properties and effective interlayer melting, ultimately contributing to the development of high-performance 3D printed materials. For the highest SSQ content (5%), clear changes in the microstructure are observed, defects within a single polymer bead resulting in weakening of the structure and, consequently, a decrease in mechanical properties. The observed changes in the microstructure may be caused by SSQ agglomeration (water on SEM EDS) and microstructure separation.

Thermal analysis results

Figure 5 presents the DSC curves for the second heating cycle of the unmodified polymer as well as the obtained PLA/SSQ-SH materials. Table 2 presents the temperature data for thermal processes occurring in the material. The first heating cycle was conducted to remove the thermal memory of the composites. Three distinct temperature ranges corresponding to different phase transitions were observed on the curves. In the 59–60 °C, signals corresponding to the glass transition temperature (T_g) were detected. In the range of 85–125 °C, cold crystallization temperature (T_{cc}) was observed, while in the range of 130–160 °C, the melting temperature (T_m) was detected. These transitions are characteristic of semicrystalline polymers, such as PLA 2003D. For the modified samples, a significantly sharper and more pronounced cold crystallization peak was observed compared to the reference sample. The presence of SSQ-SH (silsesquioxane with thiol groups) has a significant effect on the crystallization process of PLA, lowering the cold crystallization temperature as the concentration of the modifier increases. For unmodified PLA, the cold crystallization temperature (T_{cc}) is 128.0 °C, while for the polymer containing 5% SSQ-SH, T_{cc} decreases to 113.4 °C (data from the second heating cycle). Moreover, the enthalpy of cold crystallization (ΔH_{cc}) significantly increases for the PLA/SSQ-SH, indicating that SSQ-SH acts as a nucleating agent, accelerating the crystallization process of PLA[38]. This suggests that the addition of SSQ-SH leads to faster formation of an ordered crystalline structure, which directly influences the mechanical and thermal properties of the material. The nucleation effect induced by SSQ-SH promotes better control over the crystallization process, which is important for applications requiring thermal stability and an optimal crystalline structure.

Mechanical properties

Impact strength

Charpy impact tests on printed samples were conducted with the impact direction perpendicular to the layer-by-layer deposition plane (Fig. 6). The study revealed that the addition of SSQ-SH significantly improves the toughness of the materials within a certain concentration range of the modifier. For the lowest concentrations of the additive, i.e., 0.25 wt% the impact strength values are similar to those of unmodified PLA. Only concentrations above 0.5 wt% of SSQ-SH significantly affect the impact strength parameter of the samples. For concentrations of

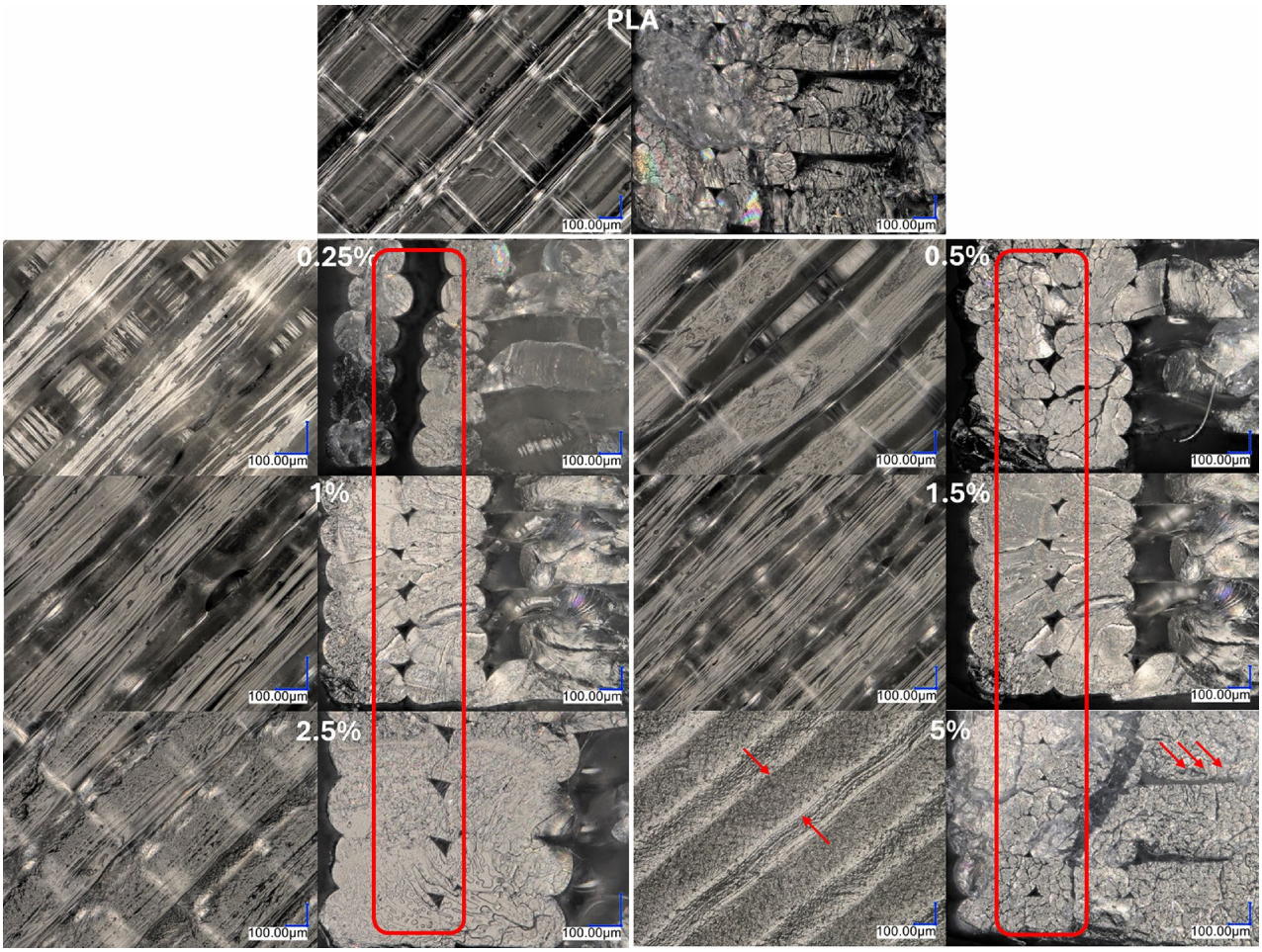

Fig. 4. Images of PLA/SSQ-SH fractures containing different wt % of the modifier after impact testing. Left-surface of bars, right-fractures.

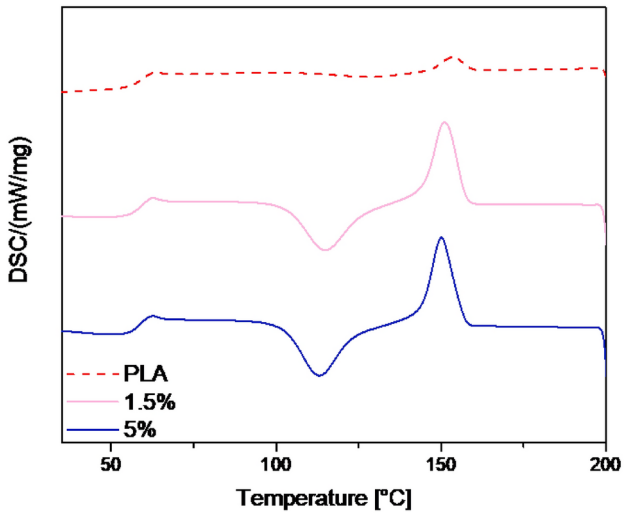

Fig. 5. DSC curves recorded for the second heating cycle.

Modifier content/cycle	T_g [°C]		T_{cc} [°C]		T_m [°C]		ΔH_{cc} [J/g]	ΔH_{cc} [J/g]
	First	Second	First	Second	First	Second	First	Second
PLA	62.0	62.9	124.5	127.6	154.5	153.9	5.1	0.8
1.5%	62.1	62.0	113.1	114.8	151.4	151.2	23.2	23.4
5%	65.5	62.1	111.0	113.4	151.1	149.9	26.7	27.0

Table 2. DSC analysis results.

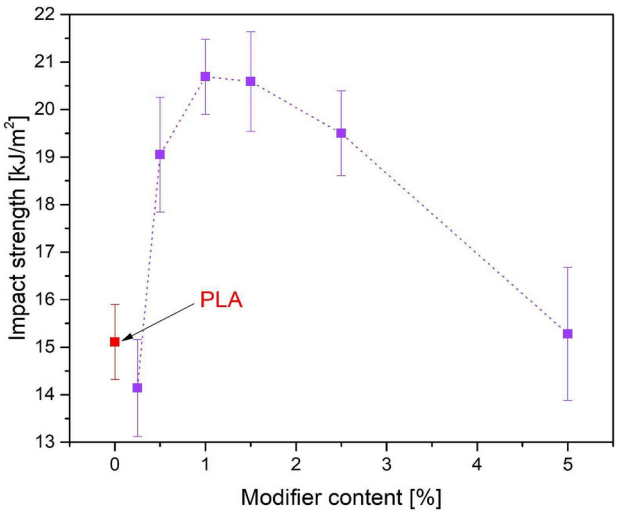

Fig. 6. Impact strength of SSQ-SH/PLA.

0.5 wt%, 1 wt%, and 1.5 wt%, the impact strength increases by approximately 26%, 37%, and 36%, respectively, compared to unmodified PLA. The addition of 2.5 wt% silsesquioxane results in a 28.4% increase compared to the reference sample. The modifier acts as a plasticizer, reducing the brittleness of the polymer, thereby allowing the materials to absorb more energy during impact. Additionally, possible interactions between -SH and -OH groups in SSQ-SH and the polymer matrix leading to the formation of hydrogen bonds, as described in our previous work[39], may also contribute to the improvement of impact strength. Despite the better processability of the samples with the highest concentration (Microscopic Analysis Sect "Mechanical properties"), its mechanical properties are not superior to PLA. The highest concentration (5 wt%) of SSQ-SH, due to limited miscibility with the polymer matrix, exceeds the capacity for uniform dispersion within the composite structure, resulting in impact strength comparable to PLA. The study indicates that optimal concentrations for the best improvement in impact properties range between 0.5 wt% and 2.5 wt% of the modifier.

Tensile strength

The results of static tensile strength tests indicate a significant increase in the flexibility of materials produced through 3D printing, attributed to the addition of SSQ-SH to the PLA matrix (Fig. 7). The elongation at break is markedly higher for modified samples, with neat PLA showing an elongation of 3.45%. Samples with concentrations ranging from 0.25 wt% to 2.5 wt% exhibit an elongation at break of 4.5% to 5%, representing a maximum increase of 56% compared to the reference PLA, particularly at concentrations of 1 wt% and 1.5 wt%. These results suggest that the added modifier acts as a plasticizer. The presence of the plasticizer enhances the "mobility" within the polymer phase. One factor affecting the mechanical properties is the penetration of the plasticizer between the macromolecular polymer chains and the increased interactions between the Si–OH groups of SSQ-SH and polylactic acid (PLA). The elongation at break for the samples containing 5 wt% (3-thiopropyl)polysilsesquioxane is similar to that of unmodified PLA, which may be due to weaker compatibility. For concentrations of 1 wt% and 1.5 wt%, an increase in tensile strength was also observed, by 9% and 10.3% respectively, compared to unmodified PLA. At concentrations of 0.1%-0.5 wt% and 2.5 wt%, tensile strength is comparable to that of neat polymer, while at 5 wt% a noticeable decrease is observed, possibly due to poorer compatibility caused by excessive modifier concentration. The increase in stress is also attributed to reinforced interactions within the polymer structure and increased crystallinity, as presented in our previous work[39]. Additionally, the Si–O–Si bonds in polysilsesquioxane are long and flexible, making the Si–O-Si chain elastic[40].

The findings suggest that samples containing 1 wt% and 1.5 wt% SSQ-SH are within an optimal concentration range, achieving a plasticizing effect that improves material flexibility while simultaneously enhancing tensile strength. The incorporation of the organosilicon compound SSQ-SH has a noticeable impact on the structure and microstructure of the polymers. This observed phenomenon may result from interactions between SSQ-SH

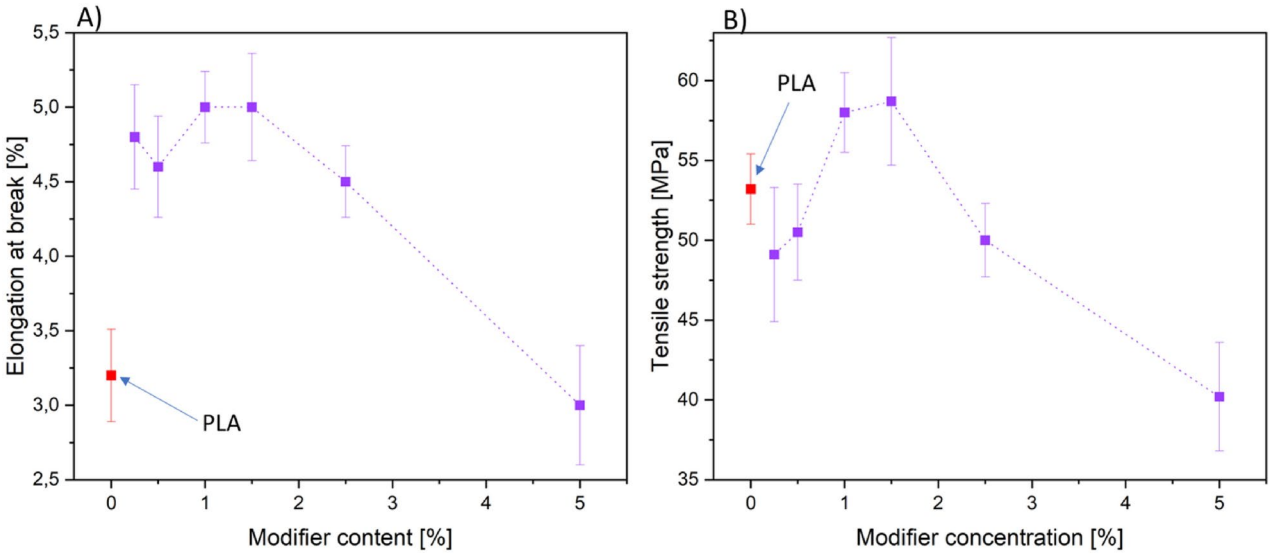

Fig. 7. (**A**) Elongation at break of SSQ-SH/PLA, (**B**) tensile strength of SSQ-SH/PLA.

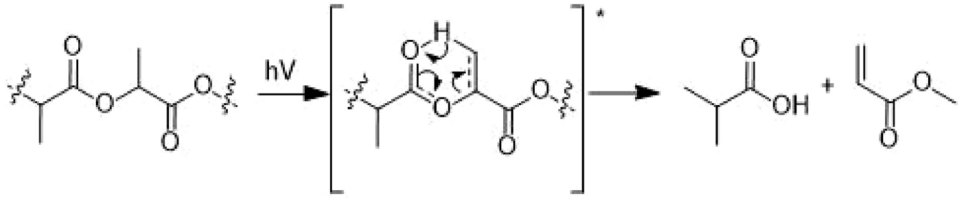

Fig. 8. Photodegradation of PLA according to the Norrish type II mechanism.

and PLA, affecting its mechanical properties. These factors are significant in the context of designing composite materials and could contribute significantly to contemporary research on polymers.

UV aging/test chamber

Fourier-transform infrared spectroscopy (FT-IR)

PLA is susceptible to photodegradation when exposed to sunlight or artificial light. This process is initiated by generating free radicals, which interact with ester bonds, leading to random chain scission within the polymer[41]. As a result of PLA degradation, molecular weight decreases, color changes, and, ultimately, there is a significant loss of the material's mechanical properties. In the presented spectra, an increase in the intensity of the signal corresponding to the elongation vibration of the ester carbonyl group after UV chamber exposure at 1750 cm^{-1} can be observed relative to the C–H signals at 1460 cm^{-1}. Moreover, the appearance of a broad band from the emerging hydroxyl bonds is also noticeable. This is associated with changes occurring in the structure of PLA due to photodegradation, resulting in the formation of new unsaturated bonds (Fig. 8). The addition of SSQ–SH does not significantly improve the stability properties of the material exposed to UV radiation, which accelerates its degradation. The differences of FTIR spectra for neat PLA and PLA/5% SSQ-SH composite are presented in Fig. 9.

Differential scanning calorimetry (DSC) after 500 h in the aging chamber

Aging tests, in which the sample is subjected to changes in temperature and humidity, affect the thermal properties of the polymer, including its crystallinity. Accelerated aging conditions at temperatures above 50 °C promote the reorganization of PLA chains, leading to its cold crystallization. Additionally, photodegradation of amorphous regions results in an increase in the relative number of crystalline regions[42]. Figure 10 A-D and Table 3 show thermograms of neat PLA and modified composites after 500 h of exposure to UV radiation. In comparison to reference samples (not subjected to aging tests), a disappearance of peaks is observed in the region associated with cold crystallization (90–120 °C), which indicates that crystallization has completely occurred during the aging process of the samples and this process does not continue. The decomposition of polymer chains promotes transformations in amorphous regions, which results in an increase in crystallinity, which is also confirmed by the X-ray diffraction patterns described in Sect "XRD analysis"[43]. This mechanism facilitates the movement of polymer chains, which leads to increased crystallinity, since the released molecular fragments in amorphous regions, due to their higher mobility, tend to rearrange into a crystalline structure[44]. In the second heating

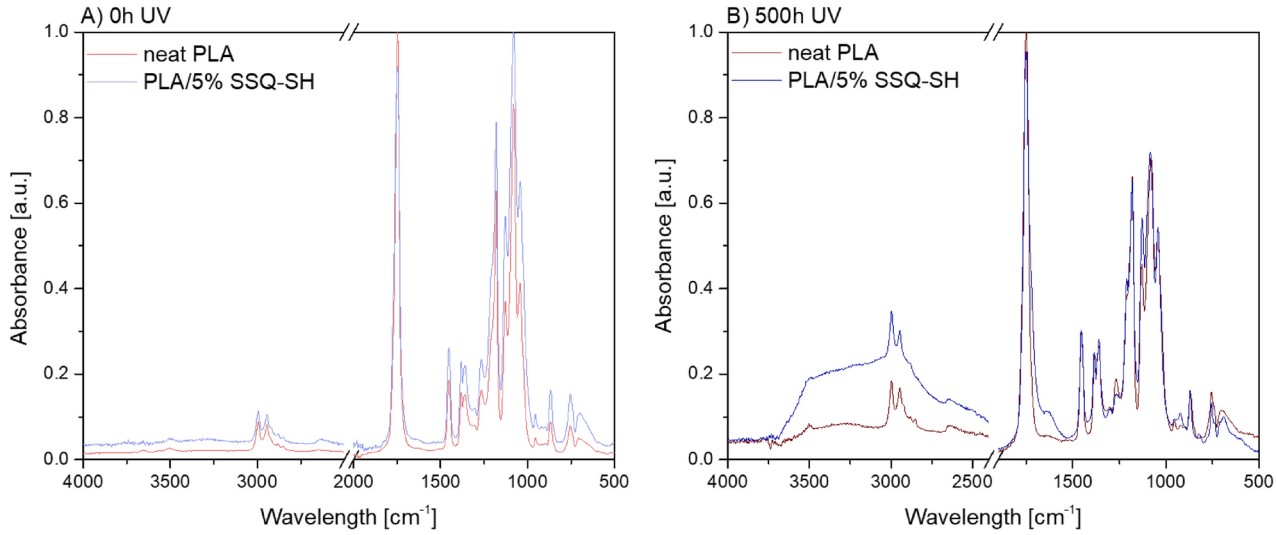

Fig. 9. The comparison of FTIR spectra for neat PLA and PLA/5% SSQ-SH composite.

cycle (Fig. 10C), three typical regions for semi-crystalline polymers are observed, which include glass transition, cold crystallization, and melting. Significant changes in the structure of the composites are visible compared to neat PLA. Both the T_{cc} and Tm peak areas are significantly larger for PLA/SH, which can be attributed to the nucleating property of the organosilicon modifier. The thermograms of the composites also show T_g in the range of 59–60 °C, recrystallization exotherm in the range of 85–110 °C and the presence of separated peaks in the melting temperature range of 130–160 °C (T_m). The reason for this may be that after the addition of SHSSQ, some of the polymer may not have fully crystallized during the initial heating or cooling. As a result, upon further heating, recrystallization occurs associated with the formation of crystallites of various shapes and sizes, small crystals that can melt at a lower temperature (first peak), while larger, more stable crystallites will melt at a higher temperature (second peak).

XRD analysis

Figure 10 shows the results of the XRD analysis of the 3D printed (Fig. 11 A) and 3D printed, and ground (Fig. 11B) samples obtained in this work after the aging process of the samples. The influence of sample aging and grinding on the results obtained was noted. A crystalline structure was seen in the XRD results of the aged samples. In addition, the effect of milling the samples can be seen in the results. In samples with (3-thiopropyl) polysilsesquioxane (SSQ-SH) that were 3D printed and then milled (Fig. 10B), a high intensity peak appeared at 2θ degrees: 16.0° ÷ 17.5° and 18.5° ÷ 19.5°. These peaks indicate the presence of a crystalline structure in the material. PLA crystallises in the form of an α phase with a rhombic structure. The 2θ positions, characteristic of this phase, correspond to two diffraction peaks: 16.3° assigned to the (200)/(110) planes and 18.65° associated with the (203) plane[45,46].

In addition, the crystallinity of the materials was calculated from the results of the XRD analysis. In Table 4, data are given for the printed samples, as the crystallinity of the powder samples was similar to each other at approximately 92%. A correlation was observed between the percentage of SSQ-SH in the samples and the crystallinity. At the lowest concentration (0.1%), the crystallinity was 70.3 ± 0.2%. As the SSQ-SH content increased to 0.25% and 0.5%, the crystallinity gradually increased to 71.7 ± 0.3% and 75.2 ± 0.2%, respectively. A more pronounced increase was observed at higher concentrations, for 1.5% SSQ-SH the crystallinity was 84.9 ± 0.3%. At the maximum concentration of SSQ-SH (5%), the crystallinity was highest at 91.4 ± 0.4%. These results indicate that SSQ-SH promotes crystallization, with the structure becoming more ordered as the additive/modifier concentration increases. A similar phenomenon was noted in the results presented in Sect "Thermal analysis results".

Optical microscopy

The microscopic images show the structure of neat PLA and modified samples (Fig. 12A–F), in which the modifier concentration was gradually increased. Clear morphological changes were observed, which are a consequence of modification and exposure to UV radiation. The reference sample, neat PLA, is characterized by a relatively smooth and uniform surface, indicating a lack of significant degradation, no significant changes in the sample structure are observed, air gaps and individual printed layers are visible, and no yellowing of the material is observed under the influence of UV radiation. In the case of samples A-F, with increasing modifier concentration, clear changes in the surface structure occur, which are manifested by an increase in the number of irregularities, cracks, and microstructural damages, the degradation of the material also caused the disappearance of clear air gaps. These observations indicate progressive degradation of the material, which is intensified in the presence of the modifier. The increase in crystallinity of samples A-F is particularly visible in the form of more irregular crystalline forms, which may be a consequence of the reorganization of the polymer structure

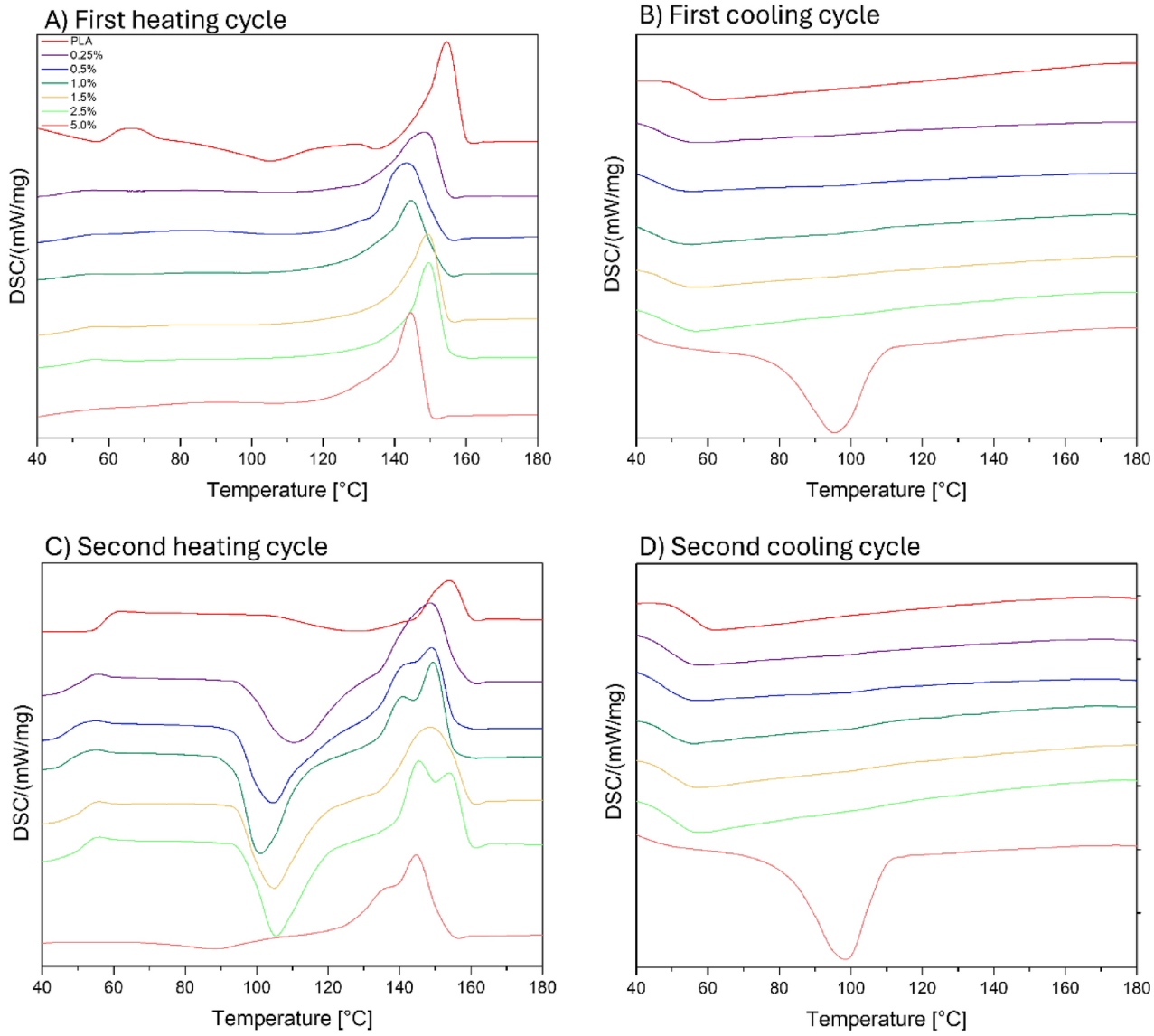

Fig. 10. DSC graphs for neat PLA and composites after conditioning in the aging chamber for 500 h.

	T_g [°C]		T_{cc} [°C]		T_m [°C]		ΔH_{cc} [J/g]	ΔH_{cc} [J/g]
Modifier content/Cycle	First	Second	First	Second	First	Second	First	Second
PLA	65.4	61.4	106.2	124.7	155.4	153.2	4.6	4.8
0.25%	53.8	54.0	–	110.4	151.8	148.6	–	32.8
0.5%	–	52.5	–	103.2	145.4	140.4/148.5	–	32.3
1.0%	–	52.8	–	101.4	147.1	141.9/150.4	–	35.3
1.5%	57.1	55.2	–	103.4	148.4	143.6/152.0	–	40.0
2.5%	56.7	55.4	–	105.2	151.7	144.4/153.1	–	41.4
5%	–	–	–	–	144.5	136.4/146.3	29.4*	23.8*

Table 3. DSC analysis results of samples after conditioning in the aging chamber for 500 h. *ΔH_c based on the cooling cycle.

due to the accelerated degradation. This is consistent with previous studies, which show that PLA degradation leads to an increase in its crystallinity due to the selective degradation of amorphous regions of the material. Furthermore, advanced stages of degradation are correlated with yellowing of the samples, especially visible in samples C-F, which indicates photodegradation of the polymer under the influence of UV radiation. These

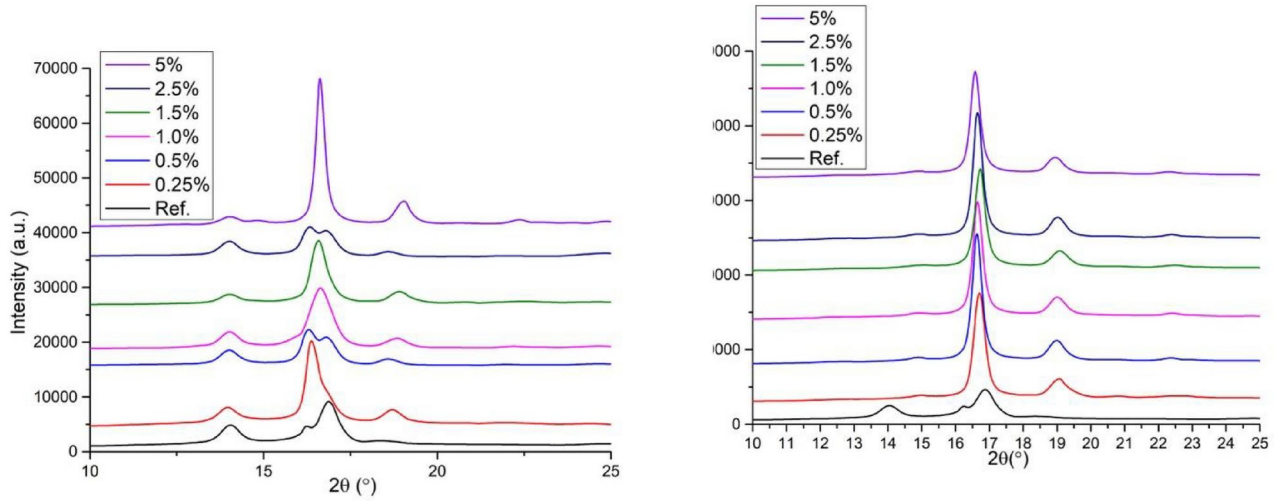

Fig. 11. X-ray diffraction (XRD) results after ageing tests: (**A**) 3D printed samples, (**B**) 3D printed and powdered samples.

Samples	Crystallinity [%]
0.25%	70.3±0.2
0.5%	71.7±0.3
1%	75.2±0.2
1.5%	77.5±0.4
2.5%	84.9±0.3
5%	91.4±0.4

Table 4. Crystallinity of the 3D printed samples after ageing tests.

samples also show significantly increased brittleness, which can be attributed to the disintegration of polymer chains, which leads to the formation of numerous structural defects. The observed morphological changes and characteristic color changes are evidence that the addition of the modifier contributes to the acceleration of the PLA degradation process, both structurally and optically.

Conclusions

The work presents a comprehensive analysis of 3D printing materials based on PLA modified with (3-thiopropyl) polysilsesquioxane (SSQ-SH). The conducted studies have shown that the modification of 3D printing materials based on PLA with the addition of (SSQ-SH) significantly improves their mechanical and structural properties. SEM–EDS microscopic analyses confirmed that SSQ-SH at lower concentrations is well dispersed in the PLA matrix, while at a concentration of 5 wt.%, it leads to the formation of larger agglomerates, which indicates a decrease in homogeneity and reduced miscibility with the PLA matrix. The addition of SSQ-SH in the range from 0.25 to 2.5 wt.% contributes to increased elasticity and strength of the material, as well as improvement of its impact properties. A significant increase in elongation at break was observed, amounting to even 56% compared to unmodified PLA, especially for samples containing from 1 to 1.5 wt.%. SSQ-SH. Charpy impact tests have shown that SSQ-SH concentrations up to 2.5 wt.% results in better energy absorption during impact and reduced material brittleness, which is particularly important for PLA-based composites. Additionally, the introduction of SSQ-SH improves interlayer melting properties, reduces the number of voids in the material, and increases its cohesion and structural integrity. This indicates the potential of this modifier in applications requiring high strength and flexibility. The optimal SSQ-SH concentrations, providing a balance between flexibility, impact resistance, and material integrity, range from 0.25 to 2.5 wt.%. Concentrations exceeding 2.5 wt.% do not provide additional mechanical benefits, and their use is not justified from a practical and economic point of view. The results of the studies emphasize the important role of optimizing additive concentrations in the design of polymer composites. SSQ-SH-modified PLA materials can be used in many areas, especially where the high brittleness of PLA is a limiting factor, especially in the production of spare parts and for maintenance purposes.

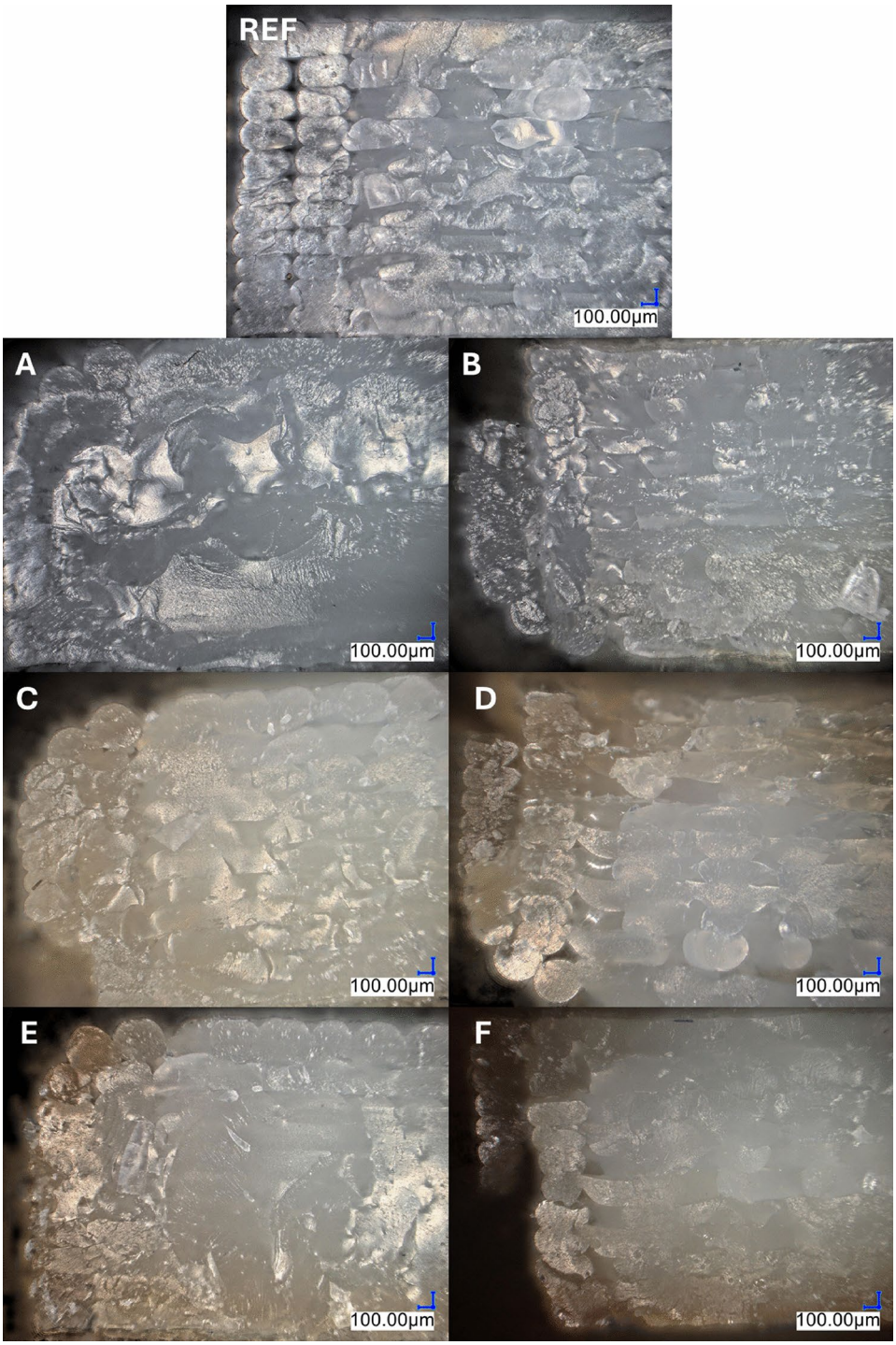

Fig. 12. The microscopic images show the structure of neat PLA and modified samples (**A**) 0.25%, (**B**) 0.5%, (**C**) 1%, (**D**) 1.5%, (**E**) 2.5%, (**F**) 5%.

Data availability

The datasets used and/or analysed during the current study are available from the corresponding author on reason-able request.

Received: 29 November 2024; Accepted: 10 January 2025
Published online: 05 March 2025

References

1. AlMaadeed, M. A. A., Ponnamma, D. & El-Samak, A. A. Polymers to improve the world and lifestyle: physical, mechanical, and chemical needs. In *Polymer Science and Innovative Applications* 1–19 (Elsevier, 2020).
2. Naser, A. Z., Deiab, I. & Darras, B. M. Poly(lactic acid) (PLA) and polyhydroxyalkanoates (PHAs), green alternatives to petroleum-based plastics: a review. *RSC Adv.* **11**, 17151–17196 (2021).
3. Taib, N. A. A. B. et al. A review on poly lactic acid (PLA) as a biodegradable polymer. *Polym. Bull.* **80**, 1179–1213 (2023).
4. Murariu, M. & Dubois, P. PLA composites: From production to properties. *Adv. Drug Deliv. Rev.* **107**, 17–46 (2016).
5. Farah, S., Anderson, D. G. & Langer, R. Physical and mechanical properties of PLA, and their functions in widespread applications—A comprehensive review. *Adv. Drug Deliv. Rev.* **107**, 367–392 (2016).
6. Subramaniam, S. R. et al. 3D printing: Overview of PLA progress. In *AIP Conference Poroceedings* (ed. Kani, B.) (AIP Publishing, 2019).
7. Steuben J, Van Bossuyt DL, Turner C. Design for Fused Filament Fabrication Additive Manufacturing. Volume 4: 20th Design for Manufacturing and the Life Cycle Conference. 9th International Conference on Micro- and Nanosystems. (2015).
8. KrishnanandTaufik, M. Fused filament fabrication (FFF) based 3D printer and its design: A review. In *Advanced Manufacturing Systems and Innovative Product Design* (eds Deepak, B. B. V. L. et al.) (Springer, 2021).
9. Ansari, A. A. & Kamil, M. Effect of print speed and extrusion temperature on properties of 3D printed PLA using fused deposition modeling process. *Mater. Today* **45**, 5462–5468 (2021).
10 MacDonald, E. & Wicker, R. Multiprocess 3D printing for increasing component functionality. *Science* https://doi.org/10.1126/science.aaf2093 (2016).
11 Macdonald, E. et al. 3D printing for the rapid prototyping of structural electronics. *IEEE Access* **2**, 234–242 (2014).
12 Gibson, I. *Additive Manufacturing Technologies 3D Printing, Rapid Prototyping, and Direct Digital Manufacturing* (Springer, 2015).
13. Siddique THM et al. Low cost 3d printing for rapid prototyping and its application. Second International Conference on Latest trends in Electrical Engineering and Computing Technologies (INTELLECT). IEEE. (2019).
14. Attaran, M. The rise of 3-D printing: The advantages of additive manufacturing over traditional manufacturing. *Bus. Horiz.* **60**, 677–688 (2017).
15. Patel, R., Desai, C., Kushwah, S. & Mangrola, M. A review article on FDM process parameters in 3D printing for composite materials. *Mater. Today* **60**, 2162–2166 (2022).
16. Sztorch, B., Brząkalski, D., Jałbrzykowski, M. & Przekop, R. E. Processing technologies for crisis response on the example of COVID-19 pandemic—Injection molding and FFF case study. *Processes* **9**, 791 (2021).
17 Radzuan, N. A. M., Sulong, A. B., Verma, A. & Muhamad, N. Layup sequence and interfacial bonding of additively manufactured polymeric composite: A brief review. *Nanotechnol. Rev.* **10**, 1853–1872 (2021).
18 Joshi, M. & Butola, B. S. Polymeric nanocomposites—Polyhedral oligomeric silsesquioxanes (POSS) as hybrid nanofiller. *J. Macromol. Sci. Part C Polym. Rev.* **44**, 389–410 (2004).
19. Phillips, S. H., Haddad, T. S. & Tomczak, S. J. Developments in nanoscience: polyhedral oligomeric silsesquioxane (POSS)-polymers. *Curr. Opin. Solid State Mater. Sci.* **8**, 21–29 (2004).
20. Brząkalski, D. et al. Why POSS-type compounds should be considered nanomodifiers, not nanofillers—A polypropylene blends case study. *Polymers* **13**, 2124 (2021).
21. Sztorch, B. et al. Trimming flow, plasticity, and mechanical properties by cubic silsesquioxane chemistry. *Sci. Rep.* https://doi.org/10.1038/s41598-023-40784-4 (2023).
22. Zhao, H. et al. Polyurethane/POSS nanocomposites for superior hydrophobicity and high ductility. *Compos. B Eng.* **177**, 107441 (2019).
23. Kozera, R. et al. Spherosilicate-modified epoxy coatings with enhanced icephobic properties for wind turbines applications. *Colloids Surf. A Physicochem. Eng.* **679**, 132475 (2023).
24. Pakuła, D., Sztorch, B., Przekop, R. E. & Marciniec, B. Click addition reaction of urethane-acrylate resin using octa(3-thiopropyl) silsesquioxane derivatives as cross-linking agents. *Processes* **11**, 3285 (2023).
25. D'Arienzo, M. et al. Unveiling the hybrid interface in polymer nanocomposites enclosing silsesquioxanes with tunable molecular structure: Spectroscopic, thermal and mechanical properties. *J. Colloid. Interface Sci.* **512**, 609–617 (2018).
26. Mishra, K., Pandey, G. & Singh, R. P. Enhancing the mechanical properties of an epoxy resin using polyhedral oligomeric silsesquioxane (POSS) as nano-reinforcement. *Polym. Test.* **62**, 210–218 (2017).
27. Hormozinezhad, F., Ehsani, M., Esmaeili, A. & Hejna, A. Combination of titanium dioxide and polyhedral oligomeric silsesquioxane nanofillers to boost mechanical and rheological properties of polyolefins: Recycling possibility. *Polym. Renew. Resour.* **15**, 25–42 (2024).
28 Kausar, A. State-of-the-art overview on polymer/POSS Nanocomposite. *Polym. Plast. Technol.* **56**, 1401–1420 (2017).
29. Omrani, A., Rostami, H. & Minaee, R. Electrochemical synthesis of polypyrrole/polyhedral oligomeric silsesquioxane nanocomposite on copper for corrosion protection. *Prog. Org. Coat.* **90**, 331–338 (2015).
30. Meyva-Zeybek, Y. & Kaynak, C. A comparative study for the behavior of 3D-printed and compression molded PLA / POSS nanocomposites. *J. Appl. Polym. Sci.* **138**, 50246 (2021).
31 Anjrini, N. et al. 3D-printed polylactic acid (PLA)/polymethyl silsesquioxane (PMSQ)-based scaffolds coated with vitamin E microparticles for the application of wound healing. *Emerg. Mater.* https://doi.org/10.1007/s42247-024-00711-3 (2024).
32. Brząkalski, D. et al. Limonene derivative of spherosilicate as a polylactide modifier for applications in 3D printing technology. *Molecules* **25**, 5882 (2020).
33. Dumitriu, A. et al. Full functionalized silica nanostructure with well-defined size and functionality: Octakis(3-mercaptopropyl) octasilsesquioxane. *J. Organomet. Chem.* **799–800**, 195–200 (2015).
34 Feher, F. J., Wyndham, K. D., Soulivong, D. & Nguyen, F. Syntheses of highly functionalized cube-octameric polyhedral oligosilsesquioxanes (R8Si8O12). *J. Chem. Soc. Dalton Trans.* **9**, 1491 (1999).
35 Pakuła, D. et al. Sulfur-containing silsesquioxane derivatives obtained by the thiol-ene reaction: synthesis and thermal degradation. *ChemPlusChem* https://doi.org/10.1002/cplu.202200099 (2022).
36. Zhu, Z., Bian, Y., Zhang, X., Zeng, R. & Yang, B. Study of crystallinity and conformation of poly (lactic acid) by terahertz spectroscopy. *Anal. Chem.* **94**(31), 11104–11111 (2022).
37. Brząkalski, D. et al. Silsesquioxane derivatives as functional additives for preparation of polyethylene-based composites: A case of trisilanol melt-condensation. *Polymers* **12**, 2269 (2020).
38. Dobrosielska, M. et al. Beeswax as a natural alternative to synthetic waxes for fabrication of PLA/diatomaceous earth composites. *Sci. Rep.* **13**, 1161 (2023).
39. Pakuła, D., Sztorch, B., Romańczuk-Ruszuk, E., Marciniec, B. & Przekop, R. E. High impact polylactide based on organosilicon nucleation agent. *Chin. J. Polym. Sci.* **42**, 787–797 (2024).
40 Luo, Ji. et al. Improving the stability and ductility of polylactic acid via phosphite functional polysilsesquioxane. *RSC Adv.* https://doi.org/10.1039/C9RA03147B (2019).
41. Copinet, A., Bertrand, C., Govindin, S., Coma, V. & Couturier, Y. Effects of ultraviolet light (315 nm), temperature and relative humidity on the degradation of polylactic acid plastic films. *Chemosphere* **55**, 763–773 (2004).
42 González-López, M. E. et al. Accelerated weathering of poly(lactic acid) and its biocomposites: A review. *Polym. Degrad. Stab.* **178**, 109290 (2020).

43. Julienne, F., Lagarde, F. & Delorme, N. Influence of the crystalline structure on the fragmentation of weathered polyolefines. *Polym. Degrad. Stab.* **170**, 109012 (2019).
44 Ahmad Sawpan, M. et al. Effect of accelerated weathering on physico-mechanical properties of polylactide bio-composites. *J. Polym. Environ.* **27**, 942–955 (2019).
45. Frone, A. N. et al. Poly(lactic acid)/Poly(3-hydroxybutyrate) biocomposites with differently treated cellulose fibers. *Molecules* **27**, 2390 (2022).
46. Saeidlou, S., Huneault, M. A., Li, H., Sammut, P. & Park, C. B. Evidence of a dual network/spherulitic crystalline morphology in PLA stereocomplexes. *Polymer* **53**, 5816–5824 (2012).

Author contributions
Conceptualization BS, methodology BS; software BS, DP, MF, TO; validation BS, REP, HS; formal analysis BS, DP, MF, ERR; investigation BS, DP, MF, TO; writing—original draft preparation BS, DP, MF, ERR; writing—review and editing BS, REP, HS; visualization BS, DP, MF, ERR; supervision BS, REP, HS; project administration BS; funding acquisition HS, BS. All authors have read and agreed to the published version of the manuscript.

Funding
This research was funded by the German Federal Ministry of Education and Research (BMBF) within the The Future of Value Creation—Research on Production, Services and Work (funding number 02P21Z000) and managed by the Project Management Agency Karlsruhe (PTKA); the National Centre for Research and Development under the LIDER X project (LIDER/01/0001/L-10/18/NCBR/2019); the Smart Growth Operational Programme, project no. POIR.04.02.00-00-D003/20-00; European Funds, project no. RPWP.01.01.00-30-0004/18; and Ministry of Science and Higher Education, project no. 21/529535/SPUB/SP/2022.

Declarations

Competing interests
The authors declare no competing interests.

Additional information
Correspondence and requests for materials should be addressed to B.S. or M.F.

Reprints and permissions information is available at www.nature.com/reprints.

Publisher's note Springer Nature remains neutral with regard to jurisdictional claims in published maps and institutional affiliations.